Eur. Phys. J. A **21**, 375–381 (2004)
DOI 10.1140/epja/i2003-10222-0

THE EUROPEAN
PHYSICAL JOURNAL A

Isospectral superdeformed bands in the N = 46 nuclei ^{88}Mo and ^{89}Tc

K. Lagergren[1,a], B. Cederwall[1], R.M. Clark[2], P. Fallon[2], A. Görgen[2,b], T. Issa[1], R.V.F. Janssens[3], A. Johnson[1], A.O. Macchiavelli[2], L. Milechina[1], D.G. Sarantites[4], and R. Wyss[1]

[1] Department of Physics, Royal Institute of Technology, SE-10691 Stockholm, Sweden
[2] Nuclear Science Division, Lawrence Berkeley National Laboratory, Berkeley, CA 94720, USA
[3] Physics Division, Argonne National Laboratory, Argonne, IL 60439, USA
[4] Department of Chemistry, Washington University, St. Louis, MO 63130, USA

Received: 1 October 2003 / Revised version: 30 January 2004 /

Communicated by D. Schwalm

Abstract. Superdeformed bands in ^{88}Mo and ^{89}Tc were populated using ^{40}Ca-induced fusion-evaporation reactions on ^{58}Ni at a beam energy of 185 MeV. Gamma-rays emitted in the reactions were detected using the Gammasphere spectrometer, in coincidence with charged particles detected by the Microball array. A new superdeformed band was assigned to the nucleus ^{88}Mo, leading to a revisit of earlier configuration assignments for superdeformed structures in this nucleus. In particular, the theoretical interpretation of a pair of identical (isospectral) superdeformed bands in ^{88}Mo/^{89}Tc is discussed. The configurations that are assigned to the four SD bands belonging to ^{88}Mo have properties that are predicted to be significantly affected by pair correlations.

PACS. 21.10.Re Collective levels – 21.60.Cs Shell model – 23.20.Lv γ transitions and level energies – 27.50.+e $59 \leq A \leq 89$

1 Introduction

The striking phenomenon of isospectral superdeformed (SD) bands has been observed in different mass regions [1]. More recently, the first case of isospectral SD bands in the $A \approx 80$ mass region have been observed [2,3]. The energies of the gamma-ray transitions between the highly excited and deformed states of two such bands belonging to different, usually neighboring, nuclei are very close to identical, and the similarity often persists over a large range in rotational frequency. The observed energy differences between the gamma-ray transitions for two such bands are sometimes within 1–2 keV, which is of the order of one per mille of the transition energies. Such extremely small energy differences are not easily explained since the addition or removal of one nucleon usually causes large deviations in the gamma-ray transition energies. Many different effects contribute to the nuclear moment of inertia, and in the large body of experimental data for SD bands throughout the nuclear chart, significant variations in the rotational moments of inertia are found. It is therefore *a priori* unlikely that the sum of all the effects on the moment of inertia will cancel when a nucleon is added to or removed from an SD nucleus. Since isospectrality is a much stricter constraint (requiring for identical moments of inertia also a given spin alignment), the likelihood that the many occurrences of isospectrality found in, *e.g.*, the $A \approx 150$ SD region are purely accidental is even smaller.

The observations of identical SD bands have stimulated a large number of theoretical efforts. These include scenarios involving pseudospin symmetry [4–6], “supersymmetry” [7] and relativistic mean-field theory [8], as well as standard cranked shell model and cranked mean-field calculations [9]. Common for most of the proposed models is the absence of quantitative predictions for the concurrence of identical moments of inertia and the proper relative spin alignment. To date no generally accepted theoretical explanation for the systematic occurrence of identical SD bands is at hand.

In the present work we present new experimental information on superdeformation in the neutron-deficient nuclei ^{88}Mo and ^{89}Tc, including the assignment of one new SD band to ^{88}Mo. A pair of isospectral SD bands in these nuclei is investigated and configuration assignments are discussed for these and the other observed SD bands.

---

[a] *Present address*: Department of Physics, Florida State University, Tallahassee, FL 32306, USA; e-mail: `karin@nuclear.kth.se`

[b] *Present address*: DAPNIA/SPhN, CEA Saclay, F-91191 Gif-sur-Yvette Cedex, France.

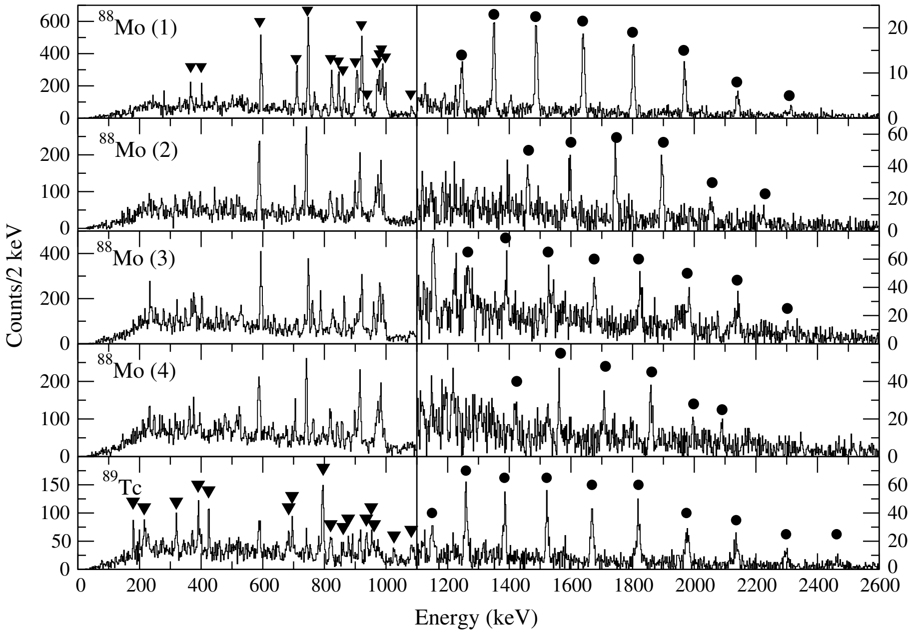

Fig. 1. The four upper panels show spectra obtained by adding all combinations of double coincidence gates on the in-band transitions of the SD bands in ^{88}Mo. For bands 1, 2 and 4, two alpha-particles and one or two protons were also required. For band 3, the stricter condition of two alpha-particles and two protons in coincidence with the gamma-rays was applied, due to the existence of the identical band in ^{89}Tc, which was the $2\alpha 1$p reaction channel in this experiment. A spectrum produced by triple gating on the transitions of that band and requiring two alpha-particles and one or zero protons is shown in the bottom panel. Note the difference in scale on the y-axis in the left and right part of the spectra. The spectra have been Doppler corrected using a variable Doppler shift as a function of gamma-ray energy, and relevant background contributions have been subtracted. The in-band gamma-ray transitions of each SD band are indicated by circles, and transitions between lower-lying states in ^{88}Mo and ^{89}Tc, respectively, are indicated by triangles.

2 The experiment

Excited states in the neutron-deficient nuclei ^{88}Mo and ^{89}Tc were populated using a ^{40}Ca ion beam impinging on a ^{58}Ni target during six days of irradiation time. The corresponding reaction channels were $2\alpha 2$p and $2\alpha 1$p, respectively. The beam, provided by the 88-Inch Cyclotron of the Lawrence Berkeley National Laboratory, had an average intensity of 4 pnA. Two different targets, consisting of 0.35 and 0.32 mg/cm^2 highly enriched ^{58}Ni on a 1 mg/cm^2 gold backing, were used. In order to minimize the shadow effect of the target frame on the charged-particle detection efficiencies, the targets were turned 10° with respect to the beam axis. Charged particles and gamma-rays emitted in the reactions were detected using the CsI(Tl) detector array Microball [10] and the Ge detector array Gammasphere [11]. Gammasphere consisted in this setup of 102 large escape-suppressed coaxial n-type Ge detectors. The targets were thin enough to allow the fusion-evaporation residues to recoil out into vacuum, and the detected gamma-rays were therefore Doppler shifted. The twofold segmentation of the 46 Ge detectors placed closest to 90° relative to the beam direction allowed for an improved Doppler correction of the detected gamma-rays. The particle identity and energy information provided by the Microball CsI detectors was used to further improve the energy resolution in the sorted gamma-ray spectra by correcting for the additional recoil caused by emission of charged particles from the compound nuclei. Heavimet collimators are normally placed in front of the BGO suppression shields that surround the Ge detectors, but in the present experiment they were removed. This was done to improve the reaction channel selectivity by applying filters on the total detected energy and gamma-ray multiplicity of every event in addition to the gating criteria on detected charged particles and gamma-rays [12,13].

Charged particles emitted from the compound nuclei, in this experiment mainly protons and alpha-particles, were identified using the pulse shapes of the scintillation signals from the 95 Microball detectors. The efficiencies for detecting and correctly identifying protons and alpha-particles were 69% and 46%, respectively, in the present experiment.

With an event trigger requiring coincidences between five or more escape-suppressed Ge detectors, around $1.4 \cdot 10^9$ raw events were stored on data tapes and analyzed off line. The data were sorted into particle-gated E_γ-E_γ-E_γ coincidence cubes, which were used to search for new superdeformed bands. The search resulted in the assignment of one new SD band to ^{88}Mo. The lifetimes of the previously known states in the SD bands in ^{88}Mo, ^{89}Tc and ^{91}Tc were also studied. These results are presented elsewhere [14].

Table 1. Transition energies for the SD bands in ^{89}Tc and ^{88}Mo observed in the present experiment. Statistical uncertainties are given within parentheses. The transition placed at the top of the SD band assigned to ^{89}Tc and the transition placed at the top of band 4 in ^{88}Mo are tentative. The SD band in ^{89}Tc and the SD band 3 in ^{88}Mo are a striking example of isospectral bands.

^{89}Tc	^{88}Mo (1)	^{88}Mo(2)	^{88}Mo (3)	^{88}Mo(4)
1149.2(3)	1238.6(4)	1459.6(8)	1260.1(12)	1418.6(9)
1258.83(11)	1342.07(23)	1595.6(7)	1382.6(13)	1560.8(10)
1384.35(7)	1480.70(23)	1743.1(5)	1522.9(17)	1706.2(9)
1521.18(8)	1633.45(22)	1894.8(5)	1668.9(16)	1858.8(9)
1668.09(6)	1795.50(25)	2054.2(9)	1817.8(15)	1995.6(14)
1818.82(8)	1962.2(3)	2224.3(16)	1975.3(14)	(2088.5(20))
1974.57(9)	2133.4(5)		2134.7(14)	
2136.01(10)	2306.5(11)		2297(3)	
2298.34(13)				
2462.0(16)				
(2619(3))				

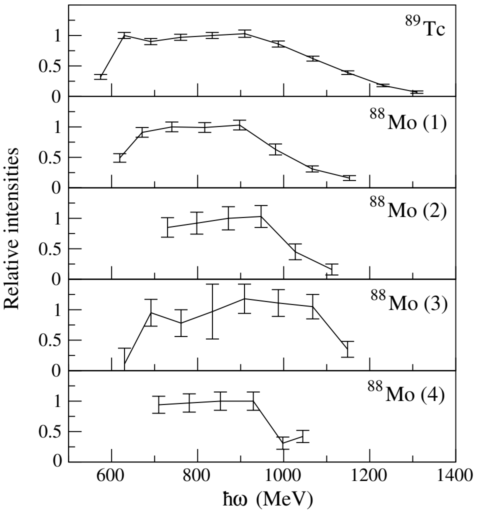

Fig. 2. Relative transition intensities of the SD bands in ^{88}Mo and ^{89}Tc as deduced from the present work, as a function of $\hbar\omega$.

3 Experimental results

Three SD bands have previously been assigned to ^{88}Mo [2] and one to ^{89}Tc [15]. The SD bands were confirmed in the present work, and one new SD band was assigned to ^{88}Mo, based on coincidences with known lower-lying transitions in ^{88}Mo [16]. No discrete gamma-ray transitions linking these bands to the lower-lying parts of the level schemes have been observed, and the absolute spins and excitation energies of the bands therefore remain unknown. The new SD band in ^{88}Mo (band 4) is populated with an intensity of around 0.3% relative to the total population of the $2\alpha 2$p reaction channel. This can be compared with the corresponding intensity of around 1% for the strongest SD band (band 1) in this nucleus. In fig. 1 are shown coincidence spectra that are double gated by the transitions in the SD bands assigned to ^{88}Mo. The measured transition energies are given in table 1, and the relative gamma-ray intensities as a function of $\hbar\omega$ are shown in fig. 2. The angular distribution ratios for band 1 in ^{88}Mo have been measured previously [2], and are consistent with the in-band transitions having a stretched quadrupole character. One should note the "identical" (isospectral) relationship between the SD band in ^{89}Tc and band 3 in ^{88}Mo. This feature was observed earlier [15], but is highlighted by the higher accuracy in the present study. The level of isospectrality is quite remarkable here; the energy differences between all the corresponding transitions in the two bands are 1–2 keV. We have ruled out the possibility that the observed gamma-ray cascades are due to proton decay competing with gamma decay at the bottom of the SD band in ^{89}Tc. The same gamma-ray sequence could then be observed in coincidence with one as well as two protons, and also with lower-lying transitions assigned to both ^{88}Mo and ^{89}Tc. The experimental data do not, however, leave room for this scenario. Protons emitted from a low-lying state in the band would be expected to follow an energy distribution with a lower mean energy than that of the protons evaporated from the "hot" compound nucleus. A search for proton decay out of band 3 did not reveal any evidence for such an effect. The search was performed by examining proton energy spectra with the requirement that two gamma-ray transitions from band 1 or band 3 of ^{88}Mo, respectively, were present in each event (the former for reference purposes), in coincidence with two alpha-particles and two protons. Band 3 in ^{88}Mo exhibits the typical intensity profile of an SD band, with a flat "plateau" in the intensity *versus* rotational-frequency curve and a rapid decay out in the low-spin part of the band. Any significant proton decay out of this band must therefore proceed via the lowest states in the band. Therefore, energy spectra for the proton with the lowest detected energy in each event were studied in particular. No qualitative differences between the proton energy spectra gated by transitions between states in the bands ^{88}Mo (3) and ^{88}Mo (1) were found.

4 Discussion

As was first pointed out by T. Bengtsson *et al.* [17], the rotational properties of SD bands systematically depend on

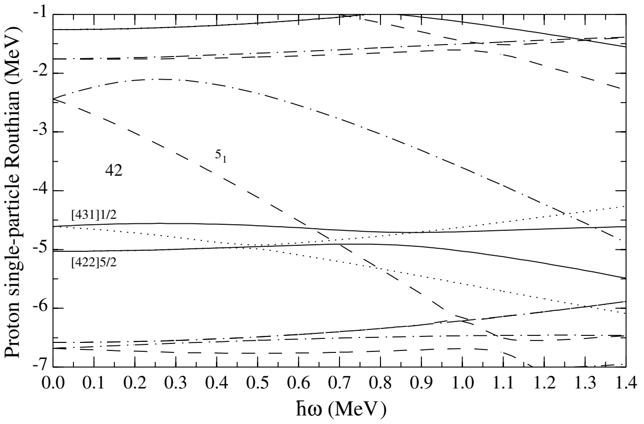

Fig. 3. Single-proton Routhians calculated for $\beta_2 = 0.488$, $\beta_4 = 0.034$, $\gamma = 2.8°$, valid around $Z = 42$. The solid lines indicate $(\pi, \alpha) = (+, +\frac{1}{2})$, dotted $(+, -\frac{1}{2})$, dash-dotted $(-, +\frac{1}{2})$, and dashed $(-, -\frac{1}{2})$. The $Z = 42$ shell gap is indicated in the figure.

the "high-$\mathcal{N}$ intruder" content of the nuclear wave function. In this context, "high-$\mathcal{N}$ intruder" denotes high-j orbitals emanating from major spherical shells above the Fermi surface which are downsloping in energy as a function of increasing quadrupole deformation. The classification of SD bands according to the number of occupied high-$\mathcal{N}$ intruder orbitals has been quite successful. However, it has also been demonstrated that in the presence of pair correlations, this simple picture needs to be modified due to the alignment of quasiparticles [18]. In particular, in the $A \approx 190$ region, paired alignment is of greater importance for the change in the moment of inertia than the number of intruder orbitals [19].

Self-consistent mean-field calculations [20,21] based on a Woods-Saxon potential and the Lipkin-Nogami pairing formalism were performed in order to interpret the experimental information on superdeformation in ^{88}Mo and ^{89}Tc. For protons in ^{88}Mo and ^{89}Tc, the orbitals predicted to be closest to the Fermi surface at SD shapes are those with the asymptotic Nilsson quantum numbers $[431]\frac{1}{2}$ and $[422]\frac{5}{2}$, emanating from the spherical $g_{7/2}$ and $g_{9/2}$ subshells, respectively, and the 5_1 orbital, which has $h_{11/2}$ parentage (see fig. 3). The notation 5_1 indicates that this is the lowest-lying orbital from the shell with principal quantum number 5. The energy levels originating in the $g_{7/2}$ and $h_{11/2}$ subshells have pronounced negative slopes as a function of increasing quadrupole deformation. Due to a shell gap of ≈ 1 MeV at neutron number $N = 46$, we expect only one neutron configuration to be of importance in the frequency range of interest. This configuration has two $\mathcal{N} = 5$ high-j orbitals occupied [2]. In an earlier work [2] the SD bands 1-3 in ^{88}Mo were assigned to the $\pi([431]\frac{1}{2})^{-1} \otimes 5_1$ (band 1) and $\pi([422]\frac{5}{2})^{-1} \otimes 5_1$ (bands 2 and 3) 2-quasiproton configurations, and the SD band in ^{89}Tc was assigned to the $\pi 5_1$ configuration. The isospectrality of the band in ^{89}Tc and band 3 in ^{88}Mo was, however, not addressed explicitly in the previous work. This fact, in combination with the observation of a new SD band in ^{88}Mo, has prompted a revisit of the configuration assignments for SD structures in this nucleus.

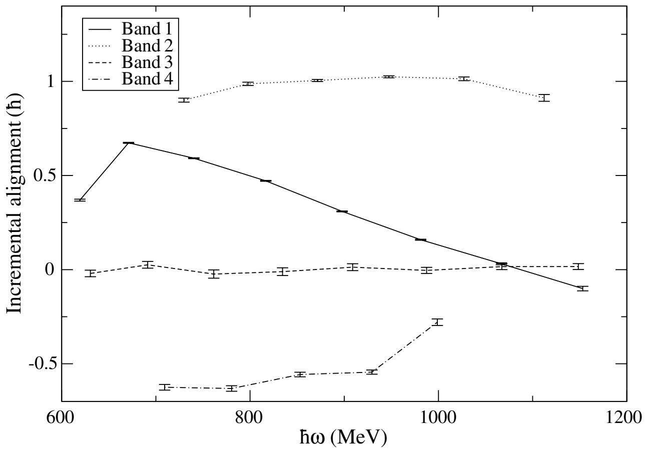

Fig. 4. Incremental alignments for the ^{88}Mo SD bands, measured relative to the SD band in ^{89}Tc. The incremental alignment is defined in the text.

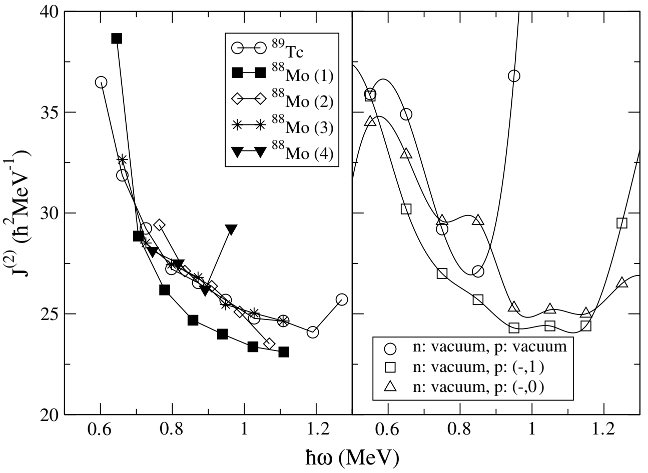

Fig. 5. Left panel: experimental $\mathcal{J}^{(2)}$ moments of inertia of the SD bands discussed in this work as a function of rotational frequency. Right panel: the corresponding curves as predicted by our calculations for the ^{88}Mo proton vacuum configuration as well as the $\pi([422]\frac{5}{2})^{-1} \otimes 5^1$ and $\pi([431]\frac{1}{2})^{-1} \otimes 5^1$ 2qp configurations.

These SD bands have a few distinct features:

i) The striking level of isospectrality of the SD band 3 in ^{88}Mo and the SD band in ^{89}Tc, as illustrated in the incremental-alignment plot of fig. 4. The incremental alignment can be deduced from the transition energies obtained in the experiment and is defined as $\Delta_i = 2\hbar\Delta E_\gamma/\Delta E_\gamma^0$, where ΔE_γ is the difference between the gamma-ray energy of a transition in a band and the transition closest to it in energy in the reference band. ΔE_γ^0 is the energy difference between two adjacent transitions in the reference band. In the present work, the SD band in ^{89}Tc is chosen as the reference.

ii) Bands 2 and 3 in ^{88}Mo have transition energies close to each other's midpoints. This is visible in the incremental-

alignment plot, where the alignment difference between the two bands is close to 1. This might point to signature partner bands built on the same strongly coupled quasiparticle (qp) configuration.
iii) The dynamical $\mathcal{J}^{(2)}$ moment of inertia values (see fig. 5) are very similar for bands 2-4 in ^{88}Mo and the band in ^{89}Tc, whereas they are significantly lower for band 1 in ^{88}Mo.

As stated above, it is reasonable to assume that the lowest SD configurations for ^{88}Mo are based on the neutron vacuum configuration ($\pi : +, \alpha : 0$); *i.e.*, a configuration lacking an excited quasineutron. In contrast, due to the large signature splitting of the lowest $\mathcal{N} = 5$ orbital, which crosses the $\mathcal{N} = 4$ orbitals at $\hbar\omega \approx 0.6\,\mathrm{MeV}$ (see fig. 3), the lowest proton configurations are based on "particle-hole excitations" from a $\mathcal{N} = 4$ orbital to $\mathcal{N} = 5$ ($\pi : -, \alpha : 0, 1$). Therefore, we expect five low-lying configurations: four proton particle-hole excitations from the $[431]\frac{1}{2}$ and $[422]\frac{5}{2}$ Nilsson orbitals into the 5_1 orbital and one based on the proton zero qp configuration ($\pi : +, \alpha : 0$). For the latter configuration, the proton intruder 5_1 orbital is empty at low frequencies. This configuration is crossed at $\hbar\omega \approx 1\,\mathrm{MeV}$ by a configuration with two aligned protons in this orbital.

The isospectrality of band 3 in ^{88}Mo and the band in ^{89}Tc places several constraints on configuration assignments. Due to the pronounced shell gap at $Z = 43$, we will here consider ^{89}Tc as the "core" nucleus (in the notation of the particle-rotor model) and the different bands in ^{88}Mo then involve different proton "hole" configurations relative to this core. Isospectral bands have been observed in particular in the $A = 150$ region. These bands have been explained in terms of the odd particle occupying an orbital with a decoupling factor of exactly $a = 1$ [6,22,23], *i.e.* contributing $\frac{1}{2}\hbar$ to the alignment relative to the core. For ^{88}Mo, no such orbitals are available close to the Fermi surface. Furthermore, an additional constraint is placed by the properties of the SD band 2, which has transition energies near the "half-points" of band 3 (*i.e.* an incremental alignment of close to 1 unit relative to band 3) in ^{88}Mo. Hence, the two constraints appear to contradict each other requiring that the configuration is both i) decoupled and ii) strongly coupled.

In the following we propose an interpretation that resolves these apparently contradicting results. Two extreme cases are usually considered for identical bands; full decoupling generating isospectral bands or bands at the midpoints of the even-even "core", and strongly coupled bands, lying at the quarter points or three-quarter points with respect to the core. In order to account for the remarkable behavior of bands 2 and 3, we here propose a third scenario based on the midshell orbital $[422]\frac{5}{2}$ of $g_{9/2}$ parentage. For a single j-shell, the core rotation results in a shift of the quantization axis from the symmetry axis toward the rotation axis of the nucleus. In this simplified picture, the midshell $\Omega = 5/2$ levels will asymptotically acquire an alignment of $\pm 1/2$ at high rotational frequencies. For ^{88}Mo, the band resulting from a proton particle-hole excitation from the negative signature of the $[422]\frac{5}{2}$ orbital to the 5_1 orbital has $\alpha = 0$, and can be described as resulting from a hole in the $[422]\frac{5}{2}$ orbital relative to the ^{89}Tc SD core. This orbital has an alignment that is rather close to the asymptotic value of $-1/2\hbar$ in the relevant spin region (fig. 3). A proton hole in this orbital thus provides the additional alignment necessary to reproduce the aligned spin sequence of the core nucleus, and offers an explanation for the observation of the isospectral bands. However, the positive signature of the same orbital is quite far from its asymptotic alignment of $+\frac{1}{2}$, due to mixing with other positive-parity configurations. In fact, it is close to parallel to its negative-signature partner level in the frequency range of interest (fig. 3). This results in an "accidental" difference in alignment of approximately one unit between the bands based on the two signatures of this orbital, in agreement with the experimental alignment difference (fig. 4) between bands 2 and 3. Furthermore, the slight curvature that is present for band 2 in the incremental-alignment plot can be ascribed to a change in alignment with rotational frequency for the $\alpha = +1/2$ signature of the $[422]\frac{5}{2}$ orbital. Hence, we assign bands 2 and 3 in ^{88}Mo to the configuration resulting from a proton particle-hole excitation into the 5_1 orbital from the positive and negative signatures of the $[422]\frac{5}{2}$ orbital, respectively. To our knowledge, this would be the first experimental example of a band exhibiting both the phenomena i) and ii) above. One should also note that the $[422]\frac{5}{2}$ orbital has very little polarizing effect on the nuclear shape, as it is totally flat in energy as a function of quadrupole deformation, in contrast to the other orbitals near the Fermi surface. It is therefore not unreasonable to assume that a difference in the occupation number of the $[422]\frac{5}{2}$ orbital does not appreciably affect the moment of inertia, in accordance with the observations.

The $[431]\frac{1}{2}$ orbital has, due to its $\Omega = 1/2$ character, a large signature splitting (see fig. 3), and we expect only the positive signature of this configuration to be populated appreciably within the rotational-frequency range of interest. The particle-hole configuration based on this orbital lacks one proton in the spherical $g_{7/2}$ orbital, which is an $\mathcal{N} = 4$ intruder orbital. A band based on such a configuration can be expected to be characterized by a lower moment of inertia than the bands based on an odd particle in the spherical $g_{9/2}$ orbital, where two $g_{7/2}$ orbitals are occupied. The difference between the moments of inertia of configurations built on orbitals of $g_{7/2}$ and $g_{9/2}$ origin are maintained in the calculations irrespectively of whether pair correlations are present and hence reflect the difference in $\mathcal{N} = 4$ intruder content.

As mentioned above, the moments of inertia of SD bands can usually be characterized quite successfully in terms of the number of occupied intruder orbitals. On the other hand, pair correlations strongly influence the moment of inertia. Our calculations show that pair correlations continue to play a role up to $\approx 1\,\mathrm{MeV}$ in rotational frequency. As shown in fig. 6, the positive-parity configurations align at $\hbar\omega \approx 1.1\,\mathrm{MeV}$. However, the interaction in the crossing regime is very strong ($> 1\,\mathrm{MeV}$). Therefore, in the presence of pairing we expect these orbitals

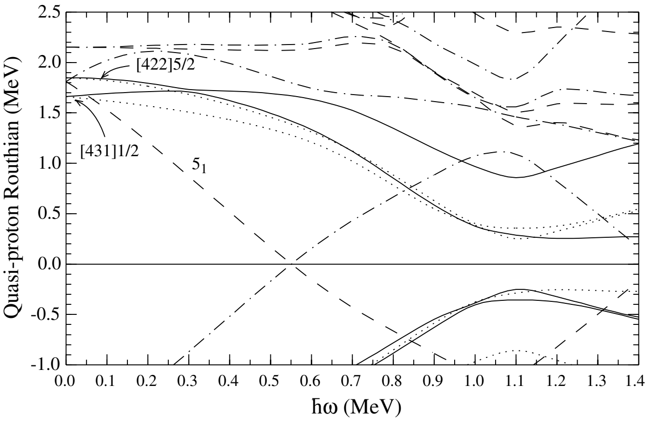

Fig. 6. Theoretical quasiparticle Routhians calculated for a Woods-Saxon potential and including quadrupole pairing as a function of rotational frequency. The calculations were made at a deformation of ($\beta_2 = 0.488$, $\beta_4 = 0.034$, $\gamma = 2.8°$). The pairing equations were solved self-consistently at each frequency. The resulting drop in the pair gap starting at $\omega \approx 0.6$ leads to a change in the slope of the quasiparticle Routhians. ($\beta_2 = 0.488$, $\beta_4 = 0.034$, $\gamma = 2.8°$). (π, α): solid $= (+, +\frac{1}{2})$, dotted $= (+, -\frac{1}{2})$, dash-dotted $= (-, +\frac{1}{2})$, dashed $= (-, -\frac{1}{2})$.

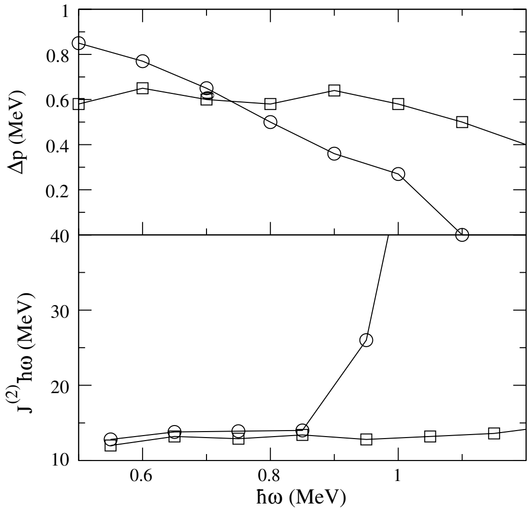

Fig. 7. Top panel: calculated proton pair gap as a function of rotational frequency for the vacuum (circles) and proton $(\pi : -, \alpha : 0)$ (squares) configurations. Bottom panel: the contribution to the $\mathcal{J}^{(2)}$ moment of inertia for the same configurations. The steeper slope in the pairing energy for the vacuum configuration compensates for the lower number of occupied intruder orbitals compared to the $(\pi : -, \alpha : 0)$ configuration, thus explaining the similarity in the $\mathcal{J}^{(2)}$ moments of inertia.

to align smoothly. The Coriolis anti-pairing effect also contributes to the increase of the moment of inertia. For the case of ^{88}Mo, the $(\pi : +, \alpha : 0)$ "proton vacuum" band has stronger proton pair correlations at low frequencies than the corresponding 2qp configurations, due to the blocking effect (see fig. 7). Due to the strong interaction between the paired and aligned positive-parity configurations, the alignment of protons in these orbitals gives rise to a smooth contribution to the $\mathcal{J}^{(2)}$ moment of inertia for the SD band with the strongest pair correlations. Furthermore, the rapid decrease in the pair gap (see fig. 7) for the vacuum band also serves to increase the $\mathcal{J}^{(2)}$ moment of inertia of the band. Consequently, although no $\mathcal{N} = 5$ orbitals are occupied in the $(\pi : +, \alpha : 0)$ configuration in the frequency range of interest, the moment of inertia of that band is boosted by the gradual alignment and decreasing pair fields. Therefore, it is as large as those of the bands built on the $\pi([422]\frac{5}{2})^{-1} \otimes 5^1$ configuration. The vacuum configuration is furthermore predicted to exhibit a sharp rise in the $\mathcal{J}^{(2)}$ moment of inertia at $\hbar\omega \approx 1\,\mathrm{MeV}$ (see fig. 5). This crossing is related to a change in configuration from $\pi 5^0$ to $\pi 5^2$. Experimentally, band 4 has a similar $\mathcal{J}^{(2)}$ moment of inertia to those of bands 2 and 3, and there is a hint of a rise in the $\mathcal{J}^{(2)}$ curve at the top of the band, which may be an indication of this band crossing. The other three bands show no signs of such band crossings at medium and high rotational frequencies. Therefore, we assign band 4 to the SD vacuum configuration.

The drop in the moment of inertia at low frequencies experienced by all the bands is calculated to originate from a paired alignment of $h_{11/2}$ neutrons. The somewhat different slopes of that alignment reflect the slightly different deformations associated with the relevant configurations.

The main features of all the observed SD bands in ^{88}Mo and ^{89}Tc are thus reproduced by our calculations, with the suggested configuration assignments.

5 Conclusions

Superdeformation in ^{88}Mo and ^{89}Tc was studied experimentally, resulting in the observation of one new SD band in ^{88}Mo as well as improved measurements of the in-band transition energies and improved values for the deduced transition quadrupole moments for three of the bands. The SD band in ^{89}Tc has previously been assigned to the $\pi 5_1$ configuration. One of the bands in ^{88}Mo (band 3) has transition energies that are very close to identical to those of the band in ^{89}Tc. In addition, band 3 appears, together with band 2 in the same nucleus, to exhibit the qualities of a strongly coupled band structure. We assign bands 2 and 3 to the positive and negative signatures of the bands resulting from a proton particle-hole excitation from the $[422]\frac{5}{2}$ orbital to the 5_1 intruder orbital, respectively. The assignment is based on the theoretically predicted alignments for these bands relative to that of the SD band in ^{89}Tc. The most intense band in the same nucleus, band 1, is assigned to the $\pi([431]\frac{1}{2})^{-1} \otimes 5_1$ configuration. The configuration assignment of the zero qp configuration depends significantly on the predicted rotational properties induced by pair correlations. The previously proposed configuration assignments of bands 1-3 in ^{88}Mo have thus been confirmed, and found to be consistent with the presence of isospectral bands. In addition, the new band observed in this work is assigned to the SD "vacuum" configuration in ^{88}Mo.

The authors would like to thank John Greene for providing targets. This work has been supported by the Swedish Research Council and by the U.S. Department of Energy through contracts Nos. W-31-109-ENG-38 (ANL), DE-FG05-88ER40406 (Washington University) and DE-AC03-76SF00093 (LBNL).

References

1. C. Baktash *et al.*, Annu. Rev. Nucl. Part. Sci. **45**, 485 (1995).
2. T. Bäck *et al.*, Eur. Phys. J. A **6**, 391 (1999).
3. F. Lerma *et al.*, Phys. Rev. C **67**, 044310 (2003).
4. F.S. Stephens *et al.*, Phys. Rev. Lett. **65**, 301 (1990).
5. F.S. Stephens *et al.*, Phys. Rev. C **57**, R1565 (1998).
6. P. Fallon, W. Nazarewicz, P.J. Twin, J.D. Garrett, Phys. Rev. Lett. **64**, 1654 (1990).
7. Yu xin Liu, Phys. Rev. C **58**, 900 (1998).
8. J. König, P. Ring, Phys. Rev. Lett. **71**, 3079 (1993).
9. P. Fallon *et al.*, Phys. Rev. C **60**, 044301 (1999).
10. D.G. Sarantites *et al.*, Nucl. Instrum. Methods Phys. Res. A **381**, 418 (1996).
11. I.-Y. Lee, Nucl. Phys. A **520**, 641c (1990).
12. M. Devlin *et al.*, Nucl. Instrum. Methods Phys. Res. A **383**, 506 (1996).
13. C. Svensson *et al.*, Nucl. Instrum. Methods Phys. Res. A **396**, 228 (1997); **403**, 57 (1998)(E).
14. K. Lagergren *et al.*, Phys. Rev. C **68**, 064309 (2003).
15. B. Cederwall *et al.*, Eur. Phys. J A **6**, 251 (1999).
16. M. Weiszflog *et al.*, Z. Phys. A **342**, 257 (1992).
17. T. Bengtsson, I. Ragnarsson, S. Åberg, Phys. Lett. B **208**, 39 (1988).
18. R. Wyss, W. Nazarewicz, A. Johnson, Phys. Lett. B **225**, 208 (1989).
19. I.M. Hibbert *et al.*, Phys. Rev. C **54**, 2253 (1996).
20. W. Satula, R. Wyss, Phys. Scr. **T56**, 159 (1995).
21. R. Wyss, W. Satula, P. Magierski, Nucl. Phys. A **578**, 45 (1994).
22. T. Byrski *et al.*, Phys. Rev. Lett. **64**, 1650 (1990).
23. D.S. Haslip *et al.*, Phys. Rev. C **57**, 2196 (1998).